Simple decision-making model for orchard air-assisted spraying airflow

Xiang Wang[1], Yuru Feng[1], Wei Fu[2], Jiangtao Qi[3], Jianli Song[1*]

(1. *Center for Chemicals Application Technology (CCAT), College of Science, China Agricultural University, Beijing 100193, China*;
2. *College of Mechanical and Electrical Engineering, Hainan University, Haikou 570100, China*;
3. *College of Biological and Agricultural Engineering, Jilin University, Changchun 130022, China*)

Abstract: Airflow speed is one of the three factors of air-assisted spraying. Optimizing the matching model between airflow speed and target canopy characteristics is an effective way to improve the orchard precision spraying technology, as airflow can significantly affect droplet deposition and drift loss. A simple model of airflow speed was established in this study. First, air-assisted spraying experiments were carried out on a standard simulation canopy to study the airflow speed depended on canopy width, leaf area index, and porosity rate. Second, determined by Ribbon Method and verified by droplet drift data, the airflow speed through the canopy was between 0.5 m/s and 0.7 m/s. Third, multiple tests were carried out under standard simulation canopy with different characteristics, and the airflow speed model was established ultimately: with a fixed leaf area index (LAI), the relationship between canopy upwind boundary airflow speed and canopy width satisfied the exponential model ($y=ae^{bx}$), and the coefficients a and b are well related to the density of branches and leaves in the canopy. When LAI=3.456, $y=2.036e^{1.5887x}$, $R^2=0.994$; LAI=1.728, $y=1.639e^{1.445x}$, $R^2=0.972$. Orchard growers can acquire needed airflow speed through this simple model, it is quick and precise and appropriate to most growth periods of a variety of fruit trees, such as apples, pears, and vines.

Keywords: airflow speed, canopy width, porosity rate, LAI, air-assisted spraying
DOI: 10.25165/j.ijabe.20231602.6849

Citation: Wang X, Feng Y R, Fu W, Qi J T, Song J L. Simple decision-making model for orchard air-assisted spraying airflow. Int J Agric & Biol Eng, 2023; 16(2): 23–29.

1 Introduction

Air-assisted spraying technology is an advanced and efficient spraying technology recommended by the United Nations Food and Agriculture Organization (FAO). With good penetration and coverage, now this technique is widely used in orchards and field crops since it was introduced in China in the 1980s[1]. The pesticide utilization rate of orchard air-assisted sprayers can reach 30%-40%, which has increased by more than 50% compared with traditional orchard sprayers using a large amount of liquid[2]. According to previous research, pesticides are more likely to get inside a canopy assisted by airflow[3,4].

Airflow direction, airflow speed, and airflow volume are the three factors of air-assisted spraying[2,5]. Among them, the penetration and deposition effects of droplets are positively correlated through airflow speed, according to research about the influence of airflow speed variation inside the canopy on pesticide deposition from He et al.[6] Although air-assisted spraying is favorable for droplet deposition in orchards, higher wind speeds are not necessarily better. As Pergher and Gubiani[7] found that increasing airflow led to lower droplet deposition and higher ground losses. The research results of Cross et al.[8] also showed that compared with medium and high air volume, low air volume could significantly increase the liquid amount deposited on the target. This is because a strong airflow will envelop and press droplets escaping from the canopy and then cause more ground losses and drift, as well as less foliar deposition. Conversely, if the airflow speed is too slow, the assistance and stress function of airflow will be too weak to achieve the ideal deposition effects. The same results are also reported by Pascuzzi et al.[9], he carried out experiments on the canopy with two different leaf area indexes (LAI) and found that airflow speed significantly affects the pesticide amount deposited on grape leaves[9]. Hence, the airflow intensity of the air-assisted sprayer should be matched with the target canopy characteristics[7,10,11]. A good fitting between airflow speed and canopy structures has a direct positive impact on the effects of air-assisted spraying[12,13], thus it is important to adjust the airflow speed applied in accordance with the architecture, size, and LAI of the target canopy.

Precision variable application technology requires not only the accurate adjustment of dosage but also the accurate adjustment of airflow. But airflow decision-making models are merely investigated by researchers, compared with dosage decision-making systems[14,15]. The principle of terminal velocity and displacement of air volume proposed in 2008[16] is still widely used as the basis for airflow decision-making[12,17,18]. However, its calculating process is rather complicated as it is requisite to introduce the canopy cross-section air volume and its correction coefficient. The automatic profiling variable spraying machine designed by Li et al.[18] realized the local air volume adjustment based on the canopy segmentation model and air volume displacement principle. Nevertheless, the control system of the machine needs to be operated manually or automatically through C++ language on the laptop computer, which

Received date: 2021-06-21 **Accepted date:** 2022-01-14
Biographies: Xiang Wang, MS of Chemistry, research interest: air-assisted spray technology research, Email: 335276376@qq.com; **Yuru Feng**, MS of Crop Protection, research interest: application of air-assisted spray technique in strawberry pest control, Email:1073670238@qq.com; **Wei Fu**, PhD, Professor, research interest: intelligent monitoring and control technology of fruit tree intelligent pruning and fruit robot picking, Email: fuwei001@126.com; **Jiangtao Qi**, PhD, Professor, research interest: agricultural artificial intelligence and bionic perception, Email: qijiangtao@jlu.edu.cn.
***Corresponding author: Jianli Song**, PhD, Associate Professor, research interest: medicine and application technology, agricultural mechanization, air-assisted spray technology research. Tel: +86-18911403029, Email: Songjianli170@163.com.

is not application-friendly for orchardists. And this machine is also difficult to popularize as an ordinary sprayer can still work.

Due to the lack of a simple, quick, and easy-to-spread airflow speed model, few growers make changes to airflow speed or volume from the first application through to the last throughout the growing season[19]. As the season progresses and the canopy fills, a fixed airflow speed from empirical estimation adopted in most orchards, which is mismatching with the actual canopy structure (too strong for the early stage and too weak for the flourishing period), caused serious agrichemical waste and environmental pollution and also led to uneven droplet distribution inside the canopy. Hence it is still a challenge for orchardists to apply airflow speed precisely to the developing target canopy throughout the whole growing season[10].

To determine the relationship between airflow speed and canopy structure, and establish a simple, rapid, and easy-to-spread airflow decision-making model fitting for widely used sprayers, the investigation of this study was carried out by 1) operation parameter selection for single fan; 2) establishing standard simulation canopy; 3) conducting single fan air-assisted spray experiment.

2 Materials and methods

2.1 Air-assisted spraying unit

The air-assisted spraying unit (hereafter referred to as spraying unit) was adopted in this experiment, which is equivalent to one-eighth of the air delivery spray devices of the prototype designed by Li et al.[18] composing of four parts: electric fan, spraying system, bracket, and power supply as shown in Figure 1a. The electric fan consists of blades, a brushless motor, and a motor speed control system. Blades of different sizes were equipped to regulate the air outlet area, and a sensor was installed for detecting the rotating speed of the fan to accurately regulate motor speed. The spraying system was composed of nozzle mounted at the center of the air outlet, an electric diaphragm pump, spray tank, pressure gage, and pressure valve to regulate spraying pressure. The bottom of the whole unit is equipped with four universal wheels to realize the free movement of the air-assisted spraying unit. TESTO hand-held anemometer (Germany) was used to measure the airflow speed at a distance of 10 cm from the air outlet. Airflow speed was measured five times under each rotating condition, and the average values are listed in Table 1.

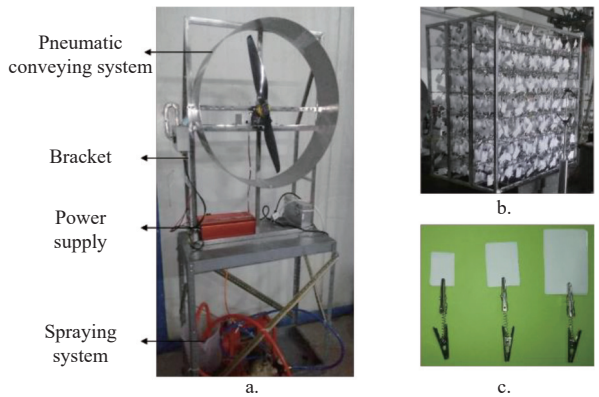

a. Air-assisted spraying unit b. Simulated canopy (Single leaf area: 24 cm², 3 frames) c. Simulated leaves of different size

Figure 1 Types of equipment used in the experiment

In this study, the atomizing angle of the nozzle is in accord with the jet angle of the axial fan, which is given by

$$\tan\alpha = 3.4\alpha \quad (1)$$

Table 1 Fan rotating speed and airflow speed with different air outlet area

Rotating speed/r·min⁻¹	Airflow speed/m·s⁻¹					
	A	B	C	D	E	F
1000	1.19	1.82	2.36	2.78	3.41	4.58
1200	1.47	2.23	2.93	3.26	4.00	5.11
1400	1.74	2.71	3.53	3.73	4.88	5.97
1600	2.01	3.13	4.07	4.41	5.46	6.71
1800	2.30	3.60	4.56	4.98	6.37	7.97
2000	2.50	4.05	5.06	5.59	7.36	8.83
2200	2.96	4.49	5.52	6.29	7.68	9.47
2400	3.30	4.92	6.03	6.99	8.50	10.32
2600	3.91	5.48	6.74	7.63	9.63	11.11
2800	4.06	5.90	7.41	8.58	10.64	12.05
3000	4.55	6.34	8.10	9.08	11.31	13.09

Note: From A to F, the area of the air outlet is 0.06, 0.09, 0.11, 0.15, 0.18, and 0.22 m², respectively; Airflow speed represents the average airflow speed at the air outlet of the fan, m/s; rotating speed represents fan rotating speed, r/min.

where, α is the polar angle and one-half of the jet angle equivalently; a is the turbulence coefficient, which is 0.12 for circular wind hood combined with axial fan, and the theoretical jet angle of the axial fan is 2α=44.30°. Hence, a hollow conical spray nozzle HCI40 (ARAG, Italy) with an atomization angle of 40° was adopted in this study.

2.2 Simulation canopy

Canopy structures of different growth periods, pruning patterns, and species vary greatly. Therefore, a standardized homogeneous simulation canopy is established.

2.2.1 Simulation canopy design

The simulation canopy is composed of branches and leaves, as well as five stainless steel frames (1.0 m×1.0 m×0.2 m). The canopy width (0.2 m-1.0 m) is adjusted by changing the frame number as shown in Figure 1b. Each frame is fixed with thin stainless steel rods (the spacing is 14.3 cm), and six simulation leaves are evenly placed on each rod. A spring attaching alligator clips to both ends mimics the twisting and swinging of branches, and three sizes of coated papers (6 cm², 12 cm², 24 cm², Figure 1c) simulate leaves at different growth periods.

2.2.2 LAI and porosity rate of simulation canopy

The LAI of the simulation canopy listed in Table 2 was calculated according to its definition[20].

Table 2 Porosity rate and LAI of simulation canopy

Simulation canopy width/m	Porosity/%		
	a	b	c
0.2	73.23	58.04	42.14
0.4	55.53	45.80	24.38
0.6	38.73	18.42	12.58
0.8	25.37	15.08	7.69
1.0	21.61	13.74	4.49

Note: a, b, and c represent simulated canopy with LAI of 0.864, 1.728, and 3.456 respectively.

As shown in Figure 2, the simulation canopy was placed in front of a white background wall, illuminated by the xenon lamp, and then the projection image was processed to obtain the proportion of light passing through the canopy, that is the canopy porosity rate. The results are also listed in Table 2.

2.3 Air-assisted spraying experiment

2.3.1 Downwind and Upwind boundary airflow speed of canopy

The downwind boundary airflow speed of the canopy (V_1) was

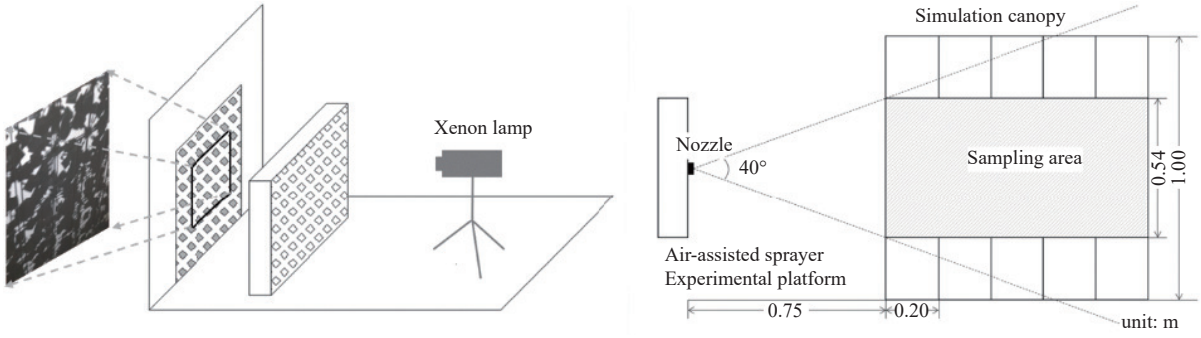

a. Porosity rate determination and image processing b. Experimental layout

Figure 2 Schematic diagram of porosity rate determination and image processing (Single leaf area: 12 cm^2, 2 layers) and experimental layout

determined by Ribbon method[21,22]. A 25 cm silk ribbon was fixed on a rod hanging naturally at a height of 1.35 m (the central axis of the fan) and just at the downwind boundary of the simulation canopy. The spraying unit is placed in front of the simulation canopy at a distance of 0.75 m, a forward speed of 0.5 m/s, and the rotating speed increased at a pace of 100 r/min gradually from 1000 r/min until the silk ribbon angle reaches 25°-40°.

The ribbon was then removed and an ultrasonic anemometer (Gill, UK, sampling frequency of 20 Hz, capable of acquiring instantaneous airflow speed and three-dimensional airflow direction) was fixed at the same position. The spraying unit was set at the same rotating speed and the corresponding airflow speed V_1 was recorded. Another ultrasonic anemometer was placed at the upwind boundary of the canopy simultaneously, 0.75 m away from the spraying unit, at a height of 1.35 m, and the upwind boundary airflow speed (V_0) presently was recorded.

The experiment was repeated three times for each canopy, and the average V_1 and V_0 are listed in Table 3.

Table 3 V_C, V_0, and V_1 of different simulation canopies

Group	LAI	L/m	P/%	Rotating speed of fan /r·min^{-1}	V_C/m·s^{-1}	V_0/m·s^{-1}	V_1/m·s^{-1}
1	0.864		73.23	1000	4.58	2.69	1.64
2	1.728	0.2	58.04	1000	4.58	2.69	1.23
3	3.456		42.14	1000	4.58	2.69	0.55
4	0.864		55.53	1000	4.58	3.01	1.15
5	1.728	0.4	45.8	1000	4.58	3.01	0.64
6	3.456		24.38	1400	5.97	3.73	0.60
7	0.864		38.73	1200	5.11	3.52	0.63
8	1.728	0.6	18.42	1300	5.66	3.84	0.64
9	3.456		12.58	1800	7.97	5.49	0.58
10	0.864		25.37	1500	6.68	4.52	0.68
11	1.728	0.8	15.08	1600	6.71	4.76	0.65
12	3.456		7.69	2300	9.68	7.35	0.59
13	0.864		21.61	1600	6.71	4.83	0.68
14	1.728	1.0	13.74	2100	9.43	7.34	0.53
15	3.456		4.49	3000	13.09	9.76	0.49

Note: V_C, V_0, and V_1 represent airflow speed at the air outlet, the upwind boundary airflow velocity, and the downwind boundary airflow velocity of canopy respectively, m/s; L is the canopy width, m; P is the canopy porosity rate.

2.3.2 Droplet escape rate test

The schematic diagram of the experimental layout is shown in Figure 2b. The spray pressure was set as 0.3 MPa, forward speed as 0.5 m/s, nozzle type CHI40015, and fan rotating speed was adjusted according to the conclusion in Section 2.3.1. At the upwind and downwind boundary of the simulation canopy, a total of 6 filter papers (diameter=7 cm) were arranged to receive droplets at the horizontal height of 1.08 m, 1.35 m, and 1.62 m, respectively, and 5% tartrazine solution was used for the test. The samples were eluted and diluted with deionized water and the absorbance value of the eluent was determined with a 722-visible spectrophotometer. The experiment was repeated three times for each canopy combination. The calculation formula is as follows:

$$W = A_1/A_0 \times 100\% \quad (2)$$

where, W represents the escape rate of droplets, %; A_1 and A_0 represent the absorbance value of the eluent of the downwind and upwind boundary of the canopy, respectively, and the results are listed in Table 4. The droplet escape rate is designed to study the feasibility of Ribbon Method and the applicable canopy range.

Table 4 Droplet escape rate (%) of different canopy combinations

Canopy width/m	Droplet escape rate/%		
	a	b	c
0.2	77.05	73.07	39.42
0.4	44.22	6.17	6.12
0.6	58.70	2.68	5.66
0.8	15.84	2.80	1.77
1.0	11.69	2.24	3.60

Note: a, b, and c represent simulated canopy with LAI of 0.864, 1.728, and 3.456, respectively. And droplet escape rate acquired of different canopy width and LAI combinations. Three groups (77.05, 73.07, and 44.22) would not work because their V_1 did not satisfy the prerequisite.

3 Results and discussion

3.1 Parameters of air-assisted spraying unit

Of the spraying unit, the brushless DC motor was equipped with blades of different sizes, and the air outlet area also changed from 0.06 m^2 to 0.22 m^2, while only 6.09 m blades with an air outlet area were 0.22 m^2, was adopted in this experiment. This is because the fan with a larger air volume is more suitable for dense fruit trees. And the fan rotating speed and the resulting airflow speed as listed in Table 1. Within the rotating speed range, the maximum airflow speed the spraying unit achieved was 13.09 m/s, which can basically meet the experimental requirements and achieve a good air-assisted spraying effect[23].

As shown in Figure 3a, the movement process of droplets in air-assisted spraying can be divided into three stages: 1) Droplets move from nozzle to the canopy; 2) Droplets enter into and deposit inside the canopy; 3) Droplets escape from the canopy.

Minimizing droplet losses in the first stage and forcing more droplets to enter the canopy are the requirements of airflow parameters adjustment. As shown in Figure 3b, when the atomizing angle of nozzle is greater than that of airflow diffusion, many droplets will get out of the wind field and deposit on the ground,

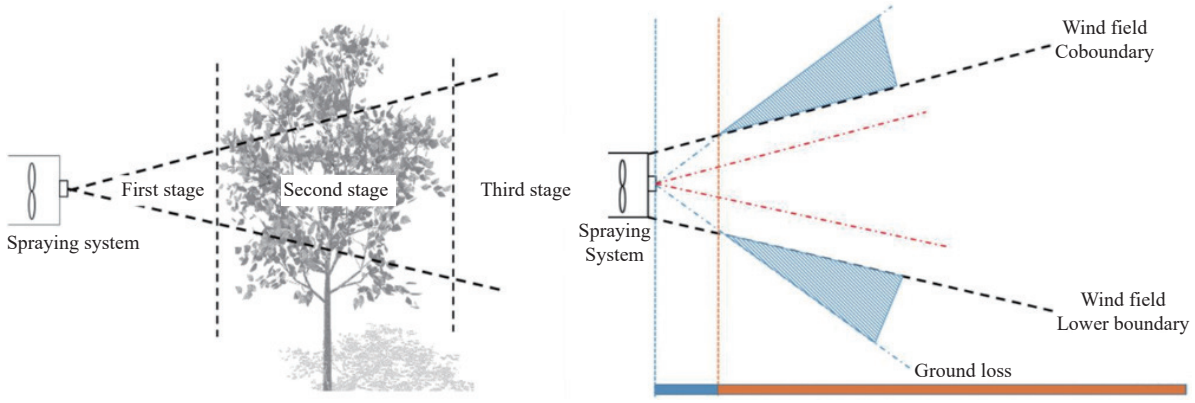

a. Three stages of droplet motion b. Jet angle of the fan and atomizing angle of the nozzle

Figure 3 Schematic diagram of the movement process of droplets and the angles comparison of droplets and airflow

thereby causing pesticide loss and environmental pollution. Furthermore, a good fitting of these two angles could reduce the influence of the external environment on droplet motion and improve its directional property. As a result, the nozzle with an atomization angle of 40° was adopted in this study. The specific parameters of the spraying unit used are listed in Table 5.

Table 5 Parameters of the spraying unit in this study

Parameter	Value
Spray pressure	0-0.6 MPa
Fan rotating speed	1000-3200 r/min
Airflow speed	4.58-13.09 m/s
Air outlet area	0.22 m²
Nozzle	HCI40015/HCI4003

Sufficient droplet deposited within the canopy and reducing the amount of droplets escaped from canopy[18] are the requirements of the second and third stage respectively. This goal was achieved by empirical Ribbon Method in this study[21,22]. Sufficient droplets within the canopy and only bits of droplets escaping from the canopy were guaranteed when the condition of the ribbon meets the requirements.

3.2 Simulation canopy parameter analysis

LAI is a dimensionless quantity that characterizes plant canopies, presenting the one-sided green leaf area per unit ground surface area in broadleaf canopies. Porosity rate is the probability of light passing through the canopy and is a key parameter to describe the canopy structure and the spatial distribution of biomass. Table 2 displays the value of LAI and the porosity rate of the simulation canopy. With a fixed LAI, the porosity rate decreases with the increase of canopy width. And similar porosity rates, such as 24.38 and 25.37, 45.80 and 42.14, may correspond to two different canopy width and LAI combinations. This rule is similar to the conclusion in homogeneous canopy established by previous scholars[24,25], a negative exponential relationship between porosity rate and the product of canopy width and LAI (hereafter referred to as $L{\cdot}W$). This indicates that the porosity rate needs to be determined by canopy width and LAI simultaneously. Canopy width is also an important characterization parameter, and it is not accurate to describe the canopy only with LAI, but not mention canopy width.

The theoretical porosity value calculated according to the mathematical relationship of the homogeneous canopy had raised by Monsi et al.[24]:

$$P = e^{-L \cdot W} \tag{3}$$

where, P is porosity rate; L represents the canopy width and W is LAI. Both theoretical and experimental porosity value are shown in Figure 4. When $L{\cdot}W$ is small, the experimental values are smaller than theoretical value, this may be ascribed to that it is difficult for the simulation canopy to be completely homogenous and leaves deviate from random distribution hypothesis. Meanwhile, the aggregation effect is not considered in this mathematical relationship. However, when $L{\cdot}W$ is relatively large, aggregation effect and random distribution hypothesis have little influence on porosity rate, as a result, theoretical and experimental values are basically the same. While porosity values from all experiments were still in line with exponential distribution, satisfying the mathematical relationship as follows:

$$\text{Porsosity} = \exp(-1.484 \cdot L \cdot W) \tag{4}$$

where, SSE of 0.068 21, R^2 of 0.8858, and RMSE of 0.0698, indicating that the simulation canopy constructed in this study basically accords with a homogeneous canopy.

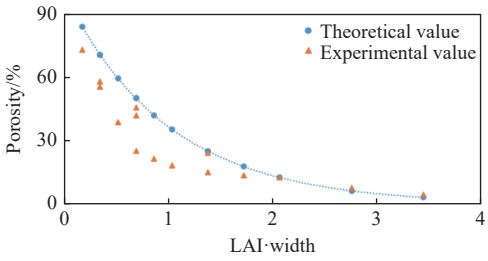

Note: The circular point is the calculated theoretical porosity value, and the triangle is the measured porosity value in the experiment.

Figure 4 Relationship of porosity with the product of LAI and canopy width

The circular point is the calculated theoretical porosity value, and the triangle is the measured porosity value in the experiment.

3.3 Exploration and sedimentary verification of airflow speed model

3.3.1 Upwind boundary airflow velocity of canopy

Landers and Vadharia[26] observed that where the air goes, the droplets will surely follow. And droplet drift was effectively reduced by adjusting airflow speed until no obvious droplets were observed behind the target canopy[27], which also proves the validity of the Ribbon method.

The values of V_1 were approximately in the range of 0.5 m/s and 0.7 m/s according to Ribbon method. Owing to the technical limitations of the spraying unit, the minimum available fan rotating speed is 1000 r/min and the corresponding airflow speed is 4.58 m/s, as listed in Table 5. When both LAI and canopy width is small,

namely, the porosity rate is large (such as in Groups 1, 2, and 4 in Table 3), the simulation canopy has a little blocking effect on airflow as well as airflow velocity cannot reach 0.7 m/s, indicating a much smaller airflow speed should be adopted in actual spraying operation for those canopies. Except for Groups 1, 2, and 4, the values of V_1 acquired from other standard canopies can meet the requirements of Ribbon method.

3.3.2 Droplet escape rate analyses

Table 4 lists droplet escape rates with different canopy widths and LAI combinations. According to Section 3.3.1, the canopy with width/LAI combinations as follows: 0.2/0.864, 0.2/1.728, and 0.4/0.864, did not meet the prerequisite: the value of V_1 was at 0.5-0.7 m/s. The droplet escape rates of canopy combinations: 0.2/3.456 and 0.6/0.864, reached 39.42%, and 58.7%. Meanwhile, droplet escape rates of canopy combinations: 0.800/0.864 and 1.000/0.864, were significantly higher than that of others, these two points indicated that the V_1 prerequisite was not applied with the canopy of too small LAI or canopy width. This is probably because canopies with small widths or LAI, in other words, relatively large canopy porosity, have a low wind-resistance coefficient. As a result, airflow will interact with the canopy to form a local flow passage and increase the local porosity rate, airflow can easily pass through the canopy and the droplet escape rate will relatively increase. This research result is similar to that of Van de Zande et al.[28] obtained on potatoes, at the early and late stages of maturity (LAI between 1 and 2), foliar deposition was 10% higher with a conventional application compared to air-assisted spraying, which may be because droplets can penetrate the canopy themselves at low LAI and high porosity canopy. Instead of increasing the leaf surface deposition, the airflow increases the probability of the droplets escaping from the canopy, leading to a significant increase in droplet escape rate. Beyond that, droplet escape rates acquired from other canopy combinations were less than 10%, indicating that Ribbon Method can still meet the principles of airflow speed decision for most canopies.

3.3.3 Upwind boundary flow velocity of canopy

As listed in Table 3, the airflow speed at the air outlet (V_C) and V_0 tend to increase gradually with the decrease of porosity rate, therefore, Pearson correlation analysis was conducted on V_C, V_0, and porosity rate (P), respectively. The analysis results showed that V_C (r=−0.814, P=0.004) and V_0 (r=−0.801, P=0.005) were both significantly correlated with porosity rate. According to the terminal velocity principle[16], that is, only airflow possessing velocity and kinetic energy of a certain amount is able to enter the canopy when it arrives at the upwind boundary. Otherwise, the airflow is blocked by the outermost canopy and cannot carry droplets into the canopy. Thus, it is more accurate and relatively straightforward to adopt the terminal velocity, namely upwind boundary airflow velocity V_0 to establish the fitting relationship between airflow speed and canopy structure compared with adopting the air outlet airflow speed, V_C.

It can be seen from Figure 5a, V_0 decreased on a logarithmic scale with the increasing porosity rate, the correlation coefficient is 0.849, which indicates a good fitting degree. However, porosity is not easy to measure in practice, while canopy width and LAI value can be easily obtained with the help of measuring equipment. In addition, the main method of tree crown detection and extraction is 3D point cloud segmentation, and the most extensive data source is lidar data[29-31]. Based on lidar data, canopy characteristic data were acquired by 3D structure reconstruction, such as tree height, canopy volume, branch length, and branching angle.

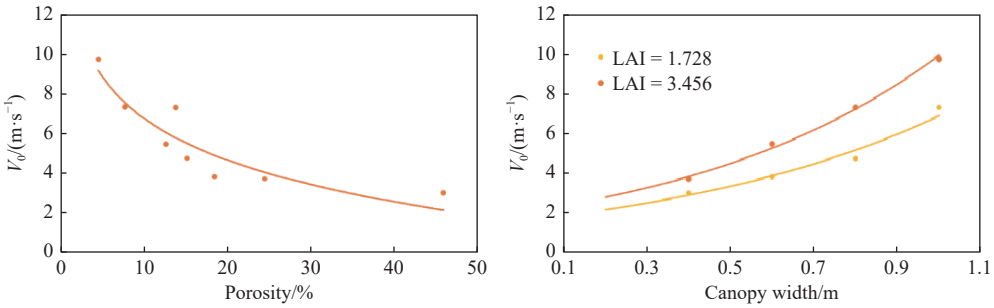

a. Regression analysis of porosity rate-V_0 b. Exponential analysis of canopy width-V_0

Note: Regression analysis was performed to porosity rate and V_0, the data were in accordance with the logarithmic curve y=−3.033ln(x)+13.75, R^2=0.849; Exponential analysis was performed to canopy width and V_0 under fixed LAI, the data were in accordance with the exponential curve y=2.036e1.5887x (LAI=3.456, R^2=0.994) and y=1.639e1.445x (LAI=1.728, R^2=0.972). The data are from groups 5 and 6, 8 and 9, 11 and 12, and 14 and 15 in Table 3.

Figure 5 The relationship of V_0 with porosity and canopy width

Moreover, based on the above conclusion of Section 3.2, under a certain LAI value, porosity decreases with the increase of canopy width, so LAI and canopy width are introduced to replace porosity to establish a mathematical relationship. When LAI are 1.728 and 3.456, data fitting curves conform to the exponential relation: y=1.639$e^{1.445x}$ and y=2.036$e^{1.5887x}$, as shown in Figure 5b. With the increase of canopy width, V_0 increased on an exponential scale, and the correlation coefficient of the curves are 0.994 and 0.972, respectively, indicating a pretty good fitting degree. According to the model, when x, i.e., canopy width, is 0, y is equal to parameter a. It seems that canopy characteristics had nothing to do with coefficient a. It is thought that for the same fan when the distance between the air outlet and canopy is certain, the coefficient a should be a constant value. However, the two values of parameter a obtained in this experiment are different, indicating that parameter a still needs to be determined through experiments for different canopies. Index b represents the growing trend of curves, $b_{LAI=1.728}$=1.445 and $b_{LAI=3.456}$=1.5887, indicating that the growth trend of V_0 is similar under the two LAI conditions. Besides, the curve growth trend of LAI=3.456 was slightly steeper than that of LAI=1.728, which may be due to the weakened degree of interaction between airflow and canopy as LAI increases. For a canopy with a constant width, the wind resistance and airflow attenuation rate increase with the LAI, which means coefficient b is closely related to LAI, and the greater the LAI is, the greater the coefficient b is.

The conclusions obtained eventually apply to many kinds of fruit trees in most growth periods, such as apples, pears, and vines.

The equation can be adapted to the middle and late stages[32,33]. While at the early stages of growth, that is, when LAI was pretty small, better spraying effects can be achieved by appropriately reducing the airflow speed or adopting a traditional sprayer without an air delivery system. In the practical application process of this conclusion, orchardists only need to offer the value of LAI of target fruit trees according to the empirical value and measure the canopy width to get the resulting airflow speed. The LAI values provided do not need to be very accurate, because in order to ensure sufficient droplet deposition, orchardists would usually increase the airflow speed applied in the field, on the basis of calculated or detecting results. In addition, since there were significant differences in LAI and especially canopy width in the vertical direction of some varieties of fruit trees, different airflow velocities should be adopted at different heights. For example, if the same airflow parameters are applied to the whole canopy of spindle trees, the airflow speed is too low for the bottom canopy to help the droplet penetrate the canopy or too high for the top canopy to cause serious droplet escaping and drifting. This demonstrated the importance and necessity of canopy width in the establishment of an airflow speed decision-making model, as well as a fixed airflow speed that will never be suitable for a whole fruit tree from top to bottom, especially for apples, pears, and such spindle-shaped fruit trees. And this conclusion is of great significance and high accuracy in the parameter adjustment, as LAI and canopy width are introduced into the model at the same time.

4 Conclusions

1) In order to study the matching relationship between air-assisted spraying parameters and canopy width, a standardized homogenous simulation canopy was designed, which could adjust LAI and canopy width to simulate fruit canopy at different growth stages and morphology. Standard canopy can eliminate differences belonging to real canopy which are hard to evaluate and quantify.

2) The Ribbon method was adopted in this study to determine the optimum airflow speed in orchard air-assisted spraying, which was validated by droplet escape test in advance. This method is suitable for most growth periods of fruit trees, except for the germination period with only a few leaves, and the escape rate of droplets is less than 7%. According to the Ribbon method, the downwind boundary airflow speed should be at 0.5-0.7 m/s.

3) The relationship between upwind boundary airflow speed V_0 and the value of porosity meet logarithmic fitting, $y=-3.033\ln(x)+13.75$, $R^2=0.849$. According to the results of the foregoing study, porosity is difficult to obtain directly and it will be more accurate and simple to introduce canopy width into the model. In the final airflow speed model, the required airflow speed is exponential to canopy width ($y=ae^{bx}$) with fixed LAI. When LAI=3.456, $y=2.036e^{1.5887x}$, $R^2=0.994$, and LAI=1.728, the relationship was $y=1.639e^{1.445x}$ and $R^2=0.972$. In this model, parameter b is closely related to LAI, and a is related to application sprayer, canopy characteristics, etc., which needs to be determined further through groups of field experiments.

4) Compared to other two decision-making model mentioned before, the final model is better in three aspects. First, the model is suitable for most growth periods of various fruit trees; Second, LAI and canopy width are introduced into the model to improve its accuracy and simplicity; The third one is also an important point in the application. After determining coefficients a and b, the model can rapidly be accepted and promptly adopted by orchardists owing to traditional air-assisted sprayers. Besides, the LAI can be inferred by combining the model with advanced LIDAR or ultrasonic technology based on the detected canopy contour data. So this model can adjust the required wind field parameters at various canopy heights in time and match the wind field with the canopy precisely. In conclusion, the model needs to achieve simple and rapid application on traditional air-assisted sprayers and also can be combined with LIDAR and infrared sensors to achieve precision variable air-assisted spraying.

Acknowledgements

The authors acknowledge that this work was financially supported by the National Natural Science Foundation of China (Grant No. 2016YFD020070). The authors also acknowledge Liu Yang's contributions to this experimental work.

[References]

[1] He X K. Research progress and developmental recommendations on precision spraying technology and equipment in China. Smart Agriculture, 2020; 2(1): 133–146. (in Chinese)

[2] Ding T H, Cao S M, Xue X Y, Ding S M. Current situation and development trend of air-assisted orchard sprayer. Journal of Chinese Agricultural Mchanization, 2016; 37(10): 221–226. (in Chinese)

[3] Michael C, Gil E, Gallart M, Kanetis L, Stavrinides M C. Evaluating the effectiveness of low volume spray application using air-assisted knapsack sprayers in wine vineyards. International Journal of Pest Management, 2020; 68(2): 148–157.

[4] An Q S, Li D, Wu Y L, Pan C P. Deposition and distribution of myclobutanil and tebuconazole in a semidwarf apple orchard by hand-held gun and air-assisted sprayer application. Pest Management Science, 2020; 76(12): 4123–4130.

[5] Zhou L F, Xue X Y, Zhou L X, Zhang L, Ding S M, Chang C, et al. Research situation and progress analysis on orchard variable rate spraying technology. Transactions of the CSAE, 2017; 33(23): 80–92. (in Chinese)

[6] He X K, Zeng A J, He J. Effect of wind velocity from orchard sprayer on droplet deposit and distribution. Transactions of CSAE, 2002; 18(4): 75–77. (in Chinese)

[7] Pergher G, Gubiani R. The effect of spray application rate and airflow rate on foliar deposition in a hedgerow vineyard. Journal of Agricultural Engineering Research, 1995; 61(3): 205–216.

[8] Corss J V, Walklate P J, Murray R A, Richardson G M. Spray deposits and losses in different sized apple trees from an axial fan orchard sprayer: 3. Effects of air volumetric flow rate. Crop Protection, 2003; 22(2): 381–394.

[9] Pascuzzi S, Cerruto E, Manetto G. Foliar spray deposition in a "tendone" vineyard as affected by airflow rate, volume rate and vegetative development. Crop Protection, 2017; 91: 34–48.

[10] Landers A J. Developments towards an automatic precision sprayer for fruit crop canopies. In: 2010 ASABE Annual International Meeting, Pittsburgh:ASABE, 2010; 1008973.

[11] Landers A J. Technologies for the precise application of pesticides into orchards and vineyards. In: 2008 ASABE Annual International Meeting, Providence:ASABE, 2008; 083727.

[12] Zhou L F, Fu X M, Ding W M, Ding S M, Chen J, Chen Z J. Design and experiment of combined disc air-assisted orchard sprayer. Transactions of the CSAE, 2015; 31(10): 64–71. (in Chinese)

[13] Pai N, Salyani M, Sweeb R D. Regulating airflow of orchard air-blast sprayer based on tree foliage density. Transactions of the ASABE, 2009; 52(5): 1423–1428.

[14] Liu H, Zhu H P, Shen Y, Chen Y, Ozkan H E. Evaluation of a laser scanning sensor for variable-rate tree sprayer development. In: 2013 ASABE Annual International Meeting, Kansas:ASABE, 2013; 2: 131594563.

[15] Gil E, Llorens J, Llop J, Fàbregas X, Escolà A, Rosell-polo J R. Variable rate sprayer. Part 2 - Vineyard prototype: Design, implementation, and validation. Computers and Electronics in Agriculture, 2013; 95: 136–150.

[16] Dai F F. Selection and calculation of the blowing rate of air-assisted sprayers. Plant Protection, 2008; 34(6): 124–127. (in Chinese)

[17] Niu C Q, Zhang W J, Wang Q, Zhao X X, Fan G J, Jiang H H. Current status and trends of research on adjusting air volume of orchard air spray. Journal of Chinese Agricultural Mechanization, 2020; 41(12): 48–54. (in

Chinese)

[18] Li L L, He X K, Song L J, Wang X N, Jia X M, Liu C H. Design and experiment of automatic profiling orchard sprayer based on variable air volume and flow rate. Transactions of the CSAE, 2017; 33(1): 70–76. (in Chinese)

[19] Landers A J, Gil E. Development and validation of a new deflector system to improve pesticide application in New York and Pennsylvania grape production areas. In:2006 ASAE Annual Meeting, ASABE, 2006; 061001.

[20] Bréda N J J. Ground-based measurements of leaf area index: A review of methods, instruments and current controversies. Journal of Experimental Botany, 2003; 54(392): 2403–2417.

[21] Deveau J. Optimizing Sprayer Air Settings - Part1. Sprayers101 n. d. Available at: https://sprayers101.com/adjust-airblast-1/. Accessed on [2021-05-10].

[22] Deveau J. Optimizing Sprayer Air Settings - Part2. Sprayers101 n. d. Available at: https://sprayers101.com/adjust-airblast-2/. Accessed on [2021-05-10].

[23] Doruchowski G, Swiechowski W, Holownicki R, Godyn A. Environmentally-dependent application system (EDAS) for safer spray application in fruit growing. The Journal of Horticultural Science and Biotechnology, 2009; 84(6): 107–112.

[24] Monsi M, Saeki T. On the factor light in plant communities and its importance for matter production. Annals of Botany, 2005; 95(3): 549–567.

[25] Monteith J L. Light distribution and photosynthesis in field crops. Annals of Botany, 1965; 29: 17–37.

[26] Landers A J, Vadharia F F. Factors influencing air and pesticide penetration into grapevine canopies. Aspects of Applied Biology, 2004; 71(2): 343–348.

[27] Palleja T, Landers A J. Real time canopy density estimation using ultrasonic envelope signals in the orchard and vineyard. Computers and Electronics in Agriculture, 2015; 115: 108–117.

[28] Van de Zande J C, Michielsen J M G P, Stallinga H, Porskamp H A J, Holterman H J, Huijsmans J F M. Environment risk control. Aspects of Applied Biology, 2002; 66: 165–176.

[29] Sanz-Cortiella R, Llorens-Calveras J, Escolà A, Arnó-Satorra J, Ribes-Dasi M, Masip-Vilalta J, et al. Innovative LIDAR 3D dynamic measurement system to estimate fruit-tree leaf area. Sensors, 2011; 11(6): 5769–5791.

[30] Zhang L, Grift T E. A LIDAR-based crop height measurement system for *Miscanthus giganteus*. Computers and Electronics in Agriculture, 2012; 85: 70–76.

[31] Sinha R, Ranjan R, Khot L R, Hoheisel G A, Grieshop M J. Comparison of within canopy deposition for a solid set canopy delivery system (SSCDS) and an axial–fan airblast sprayer in a vineyard. Crop Protection, 2020; 132: 105124.

[32] Planas S, Román C, Sanz R, Rosell-Polo J R. Bases for pesticide dose expression and adjustment in 3D crops and comparison of decision support systems. Science of The Total Environment, 2022; 806(Part1): 150357.

[33] Román C, Peris M, Esteve J, Tejerina M, Cambray J, Vilardell P, et al. Pesticide dose adjustment in fruit and grapevine orchards by DOSA3D: Fundamentals of the system and on-farm validation. Science of The Total Environment, 2022; 808: 152158.